A generalized theoretical framework to investigate multicomponent actin dynamics

Mintu Nandi*
Department of Chemistry, Indian Institute of Engineering Science and Technology, Shibpur, Howrah 711103, India

Shashank Shekhar†
Departments of Physics, Cell Biology and Biochemistry, Emory University, Atlanta, Georgia 30322, USA

Sandeep Choubey‡
The Institute of Mathematical Sciences, CIT Campus, Taramani, Chennai 600113, India and Homi Bhabha National Institute, Training School Complex, Anushaktinagar, Mumbai 400094, India

The length of actin filaments is regulated by the combined action of hundreds of actin-binding proteins. While the roles of individual proteins are well understood, how they combine to regulate actin dynamics in vivo remains unclear. Recent advances in microscopy have enabled precise, high-throughput measurements of filament lengths over time. However, the absence of a unified theoretical framework has hindered a mechanistic understanding of the multicomponent regulation of actin dynamics. To address this, we propose a general kinetic model that captures the combined effects of multiple regulatory proteins on actin dynamics. We provide closed-form expressions for both time-dependent and steady-state moments of the filament length distribution. Our framework not only differentiates between various regulatory mechanisms but also serves as a powerful tool for interpreting current data and driving future experiments.

I. INTRODUCTION

Actin filaments are key components of the cytoskeleton, driving processes such as cell motility, cytokinesis, endocytosis, and wound healing [1–3]. The regulation of filament length, essential for these processes, is controlled by a variety of actin-binding proteins (ABPs) that promote elongation, depolymerization, or capping [4–9]. While decades of biochemical research have helped elucidate the individual effects of many of these proteins, how their activities combine to drive complex actin dynamics in vivo remains poorly understood.

Recent advances in fluorescence microscopy have enabled the precise measurement of filament length changes over time for hundreds of filaments, producing rich datasets on the distribution of filament lengths as a function of time [10–13]. While numerous experimental studies have provided a wealth of data, the lack of a "theory of the experiment" [14] has hindered efforts to uncover the governing principles underlying multicomponent regulation of actin filaments.

To address this gap, we propose a general theoretical framework that captures the simultaneous effects of multiple ABPs on actin dynamics. We focus on two key aspects: (1) the time evolution of filament length distributions and (2) the steady-state distribution of filament lengths within a fixed time window. We derive exact closed-form expressions for the moments of filament length. To demonstrate the utility of this framework, we model the effects of two regulatory proteins with distinct mechanisms—an elongator (such as formin [15]) and a capper (such as capping protein [16]), both of which have been shown to simultaneously bind filament ends[17, 18]. We show that the mean and variance of filament length changes provide a powerful means to discriminate between these mechanisms. Our framework not only enables the analysis of existing experimental data but also provides a guide for designing new experiments.

II. MODEL

We develop a generalized kinetic model in which individual actin filaments can stochastically transition between different states defined by the presence of specific ABPs on filaments. In each state, filaments can polymerize, or

* mintu.rs2022@chem.iiests.ac.in
† sshekhar@emory.edu
‡ sandeep@imsc.res.in

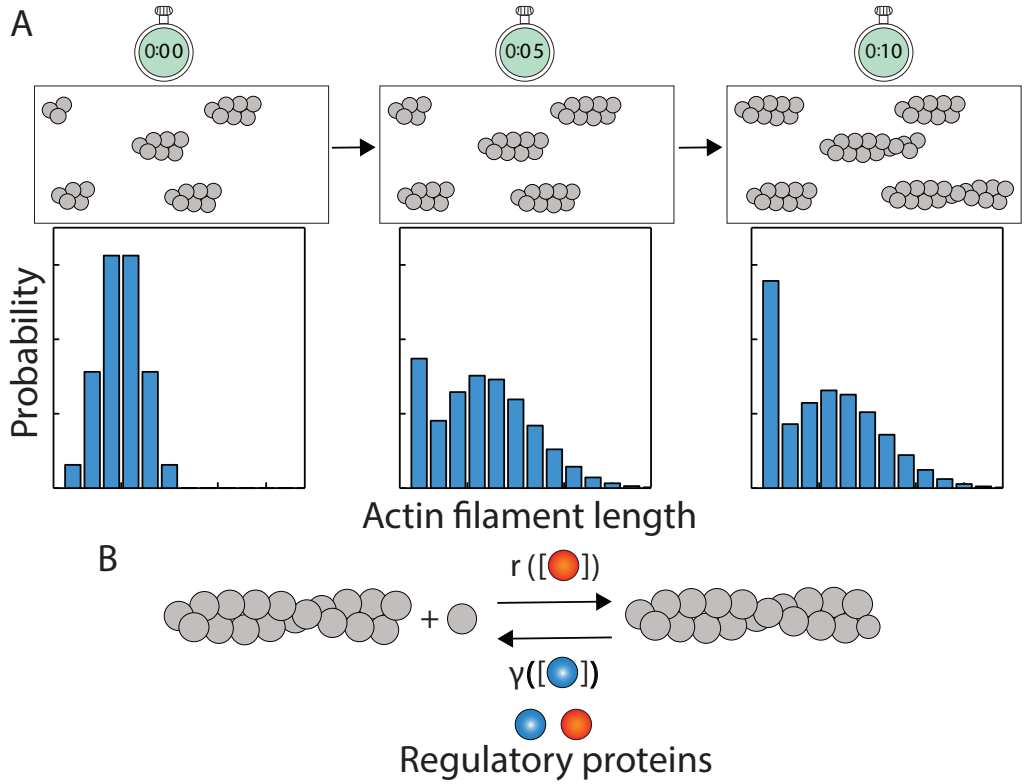

Figure 1. **Time evolution of actin filament length.** (A) Experimental time traces of actin filament length offer snapshots of the length distribution at successive time points [19–21]. (B) Effect of different regulatory proteins on actin dynamics.

depolymerize, or remain capped. Our model assumes that the filament can exist in a total of N distinct states, with N_1 states leading to polymerization and N_2 states leading to depolymerization. We consider the capped states to be part of the first cohort without any loss of generality. The rate of polymerization or depolymerization in the i-th state is given by r_i, and the transition rate from the j-th state to the i-th state is denoted by k_{ij}. Our model involves two random variables: the state of the filament i, and the change in its length, ΔL_t, over a given time interval (t). The change in length is defined as $\Delta L_t = L_t - L_0$, where L_t is the filament's length at time t and L_0 is its initial length at $t = 0$. ΔL_t can be positive (polymerization) or negative (depolymerization). We seek to compute the probability $P_i(\Delta L_t)$ that the filament's length changes by ΔL_t over a time interval t, while in the i-th state. The master equation for the time evolution of $P_i(\Delta L_t)$s in matrix form is given by

$$\frac{d}{dt}\mathbf{P}(\Delta L_t) = (\hat{\mathbf{K}} - \hat{\mathbf{R}})\mathbf{P}(\Delta L_t) + \hat{\mathbf{R}}[\mathbf{P}_{\uparrow}(\Delta L_t - 1) + \mathbf{P}_{\downarrow}(\Delta L_t + 1)], \tag{1}$$

where the probability vector $\mathbf{P}(\Delta L_t) = (P_1(\Delta L_t), \cdots, P_{N_1}(\Delta L_t), P_{N_1+1}(\Delta L_t), \cdots, P_N(\Delta L_t))^T$.
To obtain analytical solutions of Eq. (1), we introduce separate probability vectors for polymerization and depolymerization (Fig. S1). Specifically, $\mathbf{P}_{\uparrow}(\Delta L_t - 1)$ represents the probabilities of polymerizing states, and $\mathbf{P}_{\downarrow}(\Delta L_t + 1)$ represents the probabilities of depolymerizing states. The elements in $\mathbf{P}_{\uparrow}$ are zero for depolymerizing states, and vice versa for $\mathbf{P}_{\downarrow}$ (Fig. S1). The matrix $\hat{\mathbf{K}}$ in the master equation (1) describes state transitions, with off-diagonal elements k_{ij} representing the rate of transition from state j to i, and diagonal elements k_{ii} representing the outflow rate from state i (Fig. S1). The matrix $\hat{\mathbf{R}}$ is diagonal, representing the rates of polymerization and depolymerization (Fig. S1). From Eq. (1), we derive exact expressions for the moments of 1) the distribution of ΔL_t over time, and 2) the steady-state distribution of ΔL_τ within a fixed time window τ, where steady-state refers to the long-time limit where the probability distribution of ΔL_τ ceases to change.

We calculate the nth moment of the distribution of ΔL_t by multiplying both sides of Eq. (1) by ΔL_t^n. By summing over all values of ΔL_t and finally multiplying both sides by $\overrightarrow{Y} = (1, 1, \cdots, 1)_{1\times N}$, as described in the *SI text*, we

obtain the following equation for the n-th moment,

$$\begin{aligned}\langle \Delta L_t^n \rangle = &\overrightarrow{R}\left[\overrightarrow{\Lambda}_{t_\uparrow}^{(0)} + (-1)^n \overrightarrow{\Lambda}_{t_\downarrow}^{(0)}\right] \\ &+\overrightarrow{R}\sum_{x=1}^{n-1}\binom{n}{x}\left[\overrightarrow{\Lambda}_{t_\uparrow}^{(x)} + (-1)^{n+x}\overrightarrow{\Lambda}_{t_\downarrow}^{(x)}\right],\end{aligned} \tag{2}$$

where, $\overrightarrow{\Lambda}_{t_\uparrow}^{(0)} = \mathcal{L}^{-1}\left[\overrightarrow{\Delta L}_{s_\uparrow}^{(0)}/s\right]$, $\overrightarrow{\Lambda}_{t_\downarrow}^{(0)} = \mathcal{L}^{-1}\left[\overrightarrow{\Delta L}_{s_\downarrow}^{(0)}/s\right]$, $\overrightarrow{\Lambda}_{t_\uparrow}^{(x)} = \mathcal{L}^{-1}\left[\overrightarrow{\Delta L}_{s_\uparrow}^{(x)}/s\right]$, and $\overrightarrow{\Lambda}_{t_\downarrow}^{(x)} = \mathcal{L}^{-1}\left[\overrightarrow{\Delta L}_{s_\downarrow}^{(x)}/s\right]$ (see *SI text* for details). Here, $\mathcal{L}^{-1}$ denotes the inverse Laplace transformation of the partial moment vectors $\overrightarrow{\Delta L}_{s_{\cdots}}^{(\cdots)}$ defined in Laplace space s. We note here that $\overrightarrow{\Lambda}$s are obtained as functions of the matrices $\hat{\mathbf{K}}$, and $\hat{\mathbf{R}}$ (see *SI text*).

Next, we calculate the n-th moment of the steady-state distribution of ΔL_τ, given by

$$\begin{aligned}\langle \Delta L_\tau^n \rangle = &\overrightarrow{R}\left[\overrightarrow{\Delta L}_{\uparrow}^{(0)} + (-1)^n \overrightarrow{\Delta L}_{\downarrow}^{(0)}\right]\tau \\ &+\overrightarrow{R}\sum_{x=1}^{n-1}\binom{n}{x}\left[\overrightarrow{\Lambda}_{\tau_\uparrow}^{(x)} + (-1)^{n+x}\overrightarrow{\Lambda}_{\tau_\downarrow}^{(x)}\right],\end{aligned} \tag{3}$$

where, $\overrightarrow{\Lambda}_{\tau_\uparrow}^{(x)} = \mathcal{L}^{-1}\left[\frac{\overrightarrow{\Delta L}_{s_\uparrow}^{(x)}\big|_\tau}{s}\right]$, $\overrightarrow{\Lambda}_{\tau_\downarrow}^{(x)} = \mathcal{L}^{-1}\left[\frac{\overrightarrow{\Delta L}_{s_\downarrow}^{(x)}\big|_\tau}{s}\right]$ (see *SI text* for detailed analytical steps). Here, $\overrightarrow{\Delta L}_{s_{\cdots}}^{(x)}\big|_\tau$ denotes the steady-state partial moment vectors. In the above equation, $\overrightarrow{\Delta L}_{\cdots}^{(0)}$ stands for the zeroth order partial moment vectors, which characterize the occupancy of various states. The $\overrightarrow{\Lambda}$s are obtained as functions of the the matrices $\hat{\mathbf{K}}$, and $\hat{\mathbf{R}}$.

Below, we utilize our analytical results to dissect specific regulatory mechanisms of actin dynamics.

III. REGULATION OF ACTIN FILAMENT LENGTH BY A SINGLE ABP

To explore how filament growth distributions reveal mechanistic insights into multicomponent regulation of actin dynamics, we examine the combined effects of an elongator and a capper protein on filament length. Elongators promote growth [4, 5], while cappers inhibit polymerization[6]. We consider three scenarios: 1) actin filaments with only an elongator, 2) actin filaments with only a capper, and 3) actin filaments with both proteins.

A. Effect of an elongator on actin filament length

We first examined how an elongator affects actin filament length. In the presence of an elongator, the filament can exist in two states: a bare state (B) and an elongator-bound state (BF), with corresponding polymerization rates r_1 and r_2. The binding and unbinding rates of the elongator are $k_F^+ = \widetilde{k_F^+}[F]$ and k_F^-, where $[F]$ is the elongator concentration. The mean and variance of ΔL_t, as a function of time and biochemical rates, are given by

$$\begin{aligned}\langle \Delta L_t \rangle = &r_1 A_F t + r_2(1-A_F)t \\ &+\frac{(r_1-r_2)(1-A_F)}{D_F}(1-e^{-D_F t}),\end{aligned} \tag{4}$$

$$\begin{aligned}\sigma^2_{\Delta L_t} = &\frac{(r_1-r_2)(1-A_F)\left[D_F + (r_1-r_2)(1-5A_F)\right]}{D_F^2} \\ &+\left[r_2 + A_F(r_1-r_2) + \frac{2A_F(1-A_F)(r_1-r_2)^2}{D_F}\right]t \\ &-\left[\frac{(1-A_F)(r_1-r_2)}{D_F}\right]^2 e^{-2D_F t} \\ &+\frac{(1-A_F)(r_1-r_2)}{D_F^2}[4A_F(r_1-r_2) \\ &-D_F\{1+2(1-2A_F)(r_1-r_2)t\}]e^{-D_F t},\end{aligned} \tag{5}$$

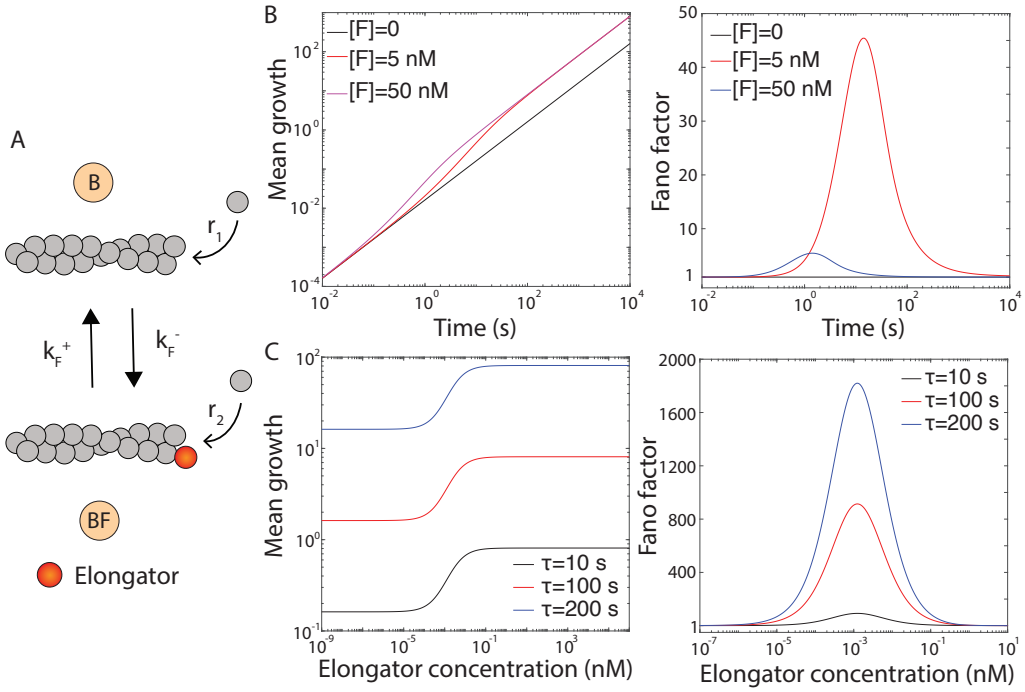

Figure 2. **Effect of an elongator on actin filament length.** (A) Two-state model of actin polymerization in the presence of elongator is illustrated. (B) Mean filament growth (μm) and Fano factor are plotted as a function of time for varying elongator concentrations. (C) Steady-state mean growth (μm) and Fano factor are shown as functions of elongator concentration for different τ values. Following parameters were used for elongator (formin): $r_1 = 6$ subunits/s, $r_2 = 30$ subunits/s, $\widetilde{k_F^+} = 29.1\,\mu M^{-1}s^{-1}$, and $k_F^- = 8.1 \times 10^{-5}$ s^{-1} [19].

where $D_F = k_F^+ + k_F^-$ and $A_F = k_F^-/D_F$. When $[F] = 0$, actin filament length increases linearly over time, driven solely by the polymerization rate of the bare (B) state (Fig. 2B). With elongator present, growth remains linear initially but becomes nonlinear at intermediate times due to the transition to the BF state. In the long term, growth is governed by the BF state polymerization rate. The Fano factor (variance over mean), which quantifies growth variability, remains at one when $[F] = 0$. In the presence of elongator, it rises above one, peaks, and then decreases, approaching one (Fig. 2B). The intermediate increase in the Fano factor reflects slow switching between the B and BF states, driven by elongator concentration.

The closed-form expressions for the steady-state mean and variance of ΔL_τ within a fixed time window τ, are given by

$$\langle \Delta L_\tau \rangle = r_1\tau + (r_1 - r_2)A_F\tau, \tag{6}$$

$$\begin{aligned}\sigma^2_{\Delta L_\tau} &= r_1\tau + (r_1 - r_2)A_F\tau \\ &\quad + \frac{2}{D_F}(r_1 - r_2)^2 A_F(1 - A_F)\tau \\ &\quad - \frac{2}{D_F^2}(r_1 - r_2)^2 A_F(1 - A_F)(1 - e^{-\tau D_F}).\end{aligned} \tag{7}$$

At steady-state, mean filament growth increases with elongator concentration, plateauing at high concentrations (Fig. 2C). The Fano factor shows nonmonotonic behavior: it remains at one at low concentrations, rises above one, peaks, and then decreases, approaching one at high concentrations (Fig. 2C). The increase at intermediate concentrations is due to slow switching between the B and BF states.

B. Effect of a capper on actin filament length

Next, we examine how a capper protein affects actin filament length. The filament can exist in two states: a bare state (B) and a capper-bound state (BC), with polymerization rates r_1 and $r_2 = 0$, respectively. The capper binding

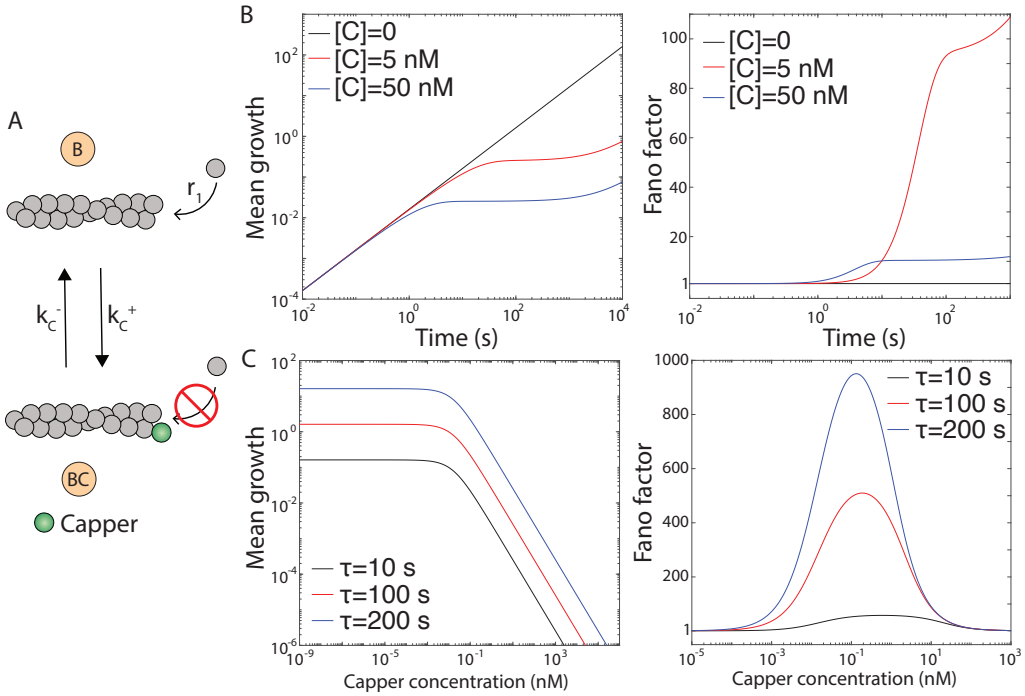

Figure 3. **Effect of a capper on actin filament length.** (A) Two-state model of actin dynamics in the presence of a capper is shown. (B) Mean filament growth (μm) and Fano factor are plotted as functions of time for different capper concentrations. (C) Steady-state mean growth (μm) and Fano factor are shown as functions of capper concentration for different values of τ. Following parameters were used for the capper(Capping protein): $r_1 = 6$ subunits/s, $\widetilde{k_C^+} = 12.8\,\mu M^{-1}s^{-1}$, and $k_C^- = 2.0 \times 10^{-4}$ s^{-1} [19].

and unbinding rates are $k_C^+ = \widetilde{k_C^+}[C]$ and k_C^-. The mean and variance of the distribution of ΔL_t are given by

$$\langle \Delta L_t \rangle = r_1 A_C t + \frac{r_1(1-A_C)}{D_C}(1 - e^{-D_C t}), \tag{8}$$

$$\begin{aligned}\sigma^2_{\Delta L_t} = {} & r_1 A_C t + \frac{2r_1^2 A_C(1-A_C)t}{D_C} \\ & + \left[\frac{r_1(1-A_C)}{D_C}\right]^2 (1 - e^{-2D_C t}) \\ & + \frac{r_1(1-A_C)}{D_C}\left(1 - \frac{2r_1}{D_C}\right)(1 - e^{-D_C t}) \\ & + \frac{2r_1^2(1-A_C)(1-2A_C)}{D_C^2} \\ & \times \left[1 - (1 + D_C t)e^{-D_C t}\right], \end{aligned} \tag{9}$$

where $D_C = k_C^+ + k_C^-$ and $A_C = k_C^-/D_C$. At $[C] = 0$, the mean growth is higher than when $[C] > 0$ (Fig. 3B). As capper concentration increases, the growth rate decreases, demonstrating an inverse relationship between $[C]$ and filament growth (Fig. 3B).

When $[C] = 0$, the Fano factor is one, and filament growth is Poissonian (Fig. 3B). Adding capper initially has no effect on growth variability, as it does not bind to the barbed end. Over time, capper binds, capping the filament and increasing the Fano factor, with a more pronounced increase at lower concentrations. The transient phase exhibits dynamic behavior due to frequent transitions between the bare (B) and capped (BC) states. In the long term, the Fano factor plateaus (Fig. 3B).

The mean and the variance of the steady-state distribution of ΔL_τ are given by

$$\langle \Delta L_\tau \rangle = r_1 A_C \tau, \tag{10}$$

$$\sigma^2_{\Delta L_\tau} = r_1 A_C \tau + \frac{2}{D_C} r_1^2 A_C (1 - A_C)\tau - \frac{2}{D_C^2} r_1^2 A_C (1 - A_C)(1 - e^{-\tau D_C}). \tag{11}$$

Mean steady-state growth is highest without capper and decreases with increasing capper concentration (Fig. 3C), as capper reduces the time filaments spend in the bare (B) state, where polymerization occurs. The Fano factor remains at one at low capper concentrations but shows non-monotonic behavior: it rises, peaks when B and BC states are equally occupied, and then returns to one (Fig. 3C). Over longer time windows, variability increases due to higher overall growth.

IV. COMBINED EFFECTS OF AN ELONGATOR AND A CAPPER ON ACTIN FILAMENT LENGTH

So far we have quantified the individual effects of an elongator or a capper. However, in cells, these factors act simultaneously, often targeting the same site on a filament[17, 18]. We consider two models to explore the combined effect of an elongator and a capper, see Fig. 4A. First, Competitive Binding Model: The elongator and capper bind the same filament end in a mutually exclusive manner. In this model, the filament can exist in three states—free (B), capper-bound (BC), or elongator-bound (BF)—with polymerization rates r_1, r_2, and $r_3 = 0$, respectively. Second, Simultaneous Binding Model: Both proteins can simultaneously bind the same filament end. Thus, the filament can now occupy four states—free (B, r_1), elongator-bound (BF, r_2), capper-bound (BC, $r_4 = 0$), or dual-bound (BFC, $r_3 = 0$).

To differentiate between the two models, we analyze steady-state variability in filament growth by varying elongator concentration at different capper concentrations (Fig. 4B). In both models, the Fano factor shows non-monotonic behavior: it rises from low values at low elongator concentrations, peaks, and then decreases at higher concentrations. In the competitive binding model, the Fano factor approaches one at high elongator concentrations, indicating Poissonian growth. In contrast, the simultaneous binding model yields a Fano factor greater than one, which increases with capper concentration. These differences reflect how state occupancy changes with elongator concentration. In the competitive model, high elongator concentrations increase occupancy of the elongator-bound state, reducing variability. In the simultaneous model, the filament alternates between two states, leading to higher variability even at high elongator concentrations.

Different mechanisms of multicomponent regulation of actin dynamics can be discriminated by the distributions of filament lengths they produce.

V. DISCUSSION

The study of actin filament dynamics has a rich experimental history, with theoretical models playing a key role in interpreting data. Two main classes of modeling efforts have emerged in this field. The first focuses on how actin filament length is regulated in steady-state conditions [22–25]. The second class of models examines the temporal aspects of filament growth [26, 27]. Notably, most of these models are computational and focus on specific mechanisms with a limited set of actin-binding proteins. In contrast, we propose a generalized analytical framework that captures the combined effects of an arbitrary number of regulatory proteins on actin filament dynamics.

So far, we have focused primarily on a single elongator and capper. However, cells contain a diverse range of regulatory factors, including depolymerases like twinfilin and cofilin [28], as well as numerous elongators and cappers such as formins [15] (with 15 mammalian isoforms) and Ena/VASP proteins [29]. Further complexity arises from the two distinct filament ends and the age of the filaments, which influence protein binding and activity. Due to its general framework, our model can accommodate these complexities, offering a more integrated understanding of actin dynamics in physiological contexts.

ACKNOWLEDGMENTS

MN acknowledges SERB, India, for the National Post-Doctoral Fellowship [PDF/2022/001807]. SS was funded by NIH NIGMS Grant No. R35GM143050. SC acknowledges the support provided by the DBT Ramalingaswami

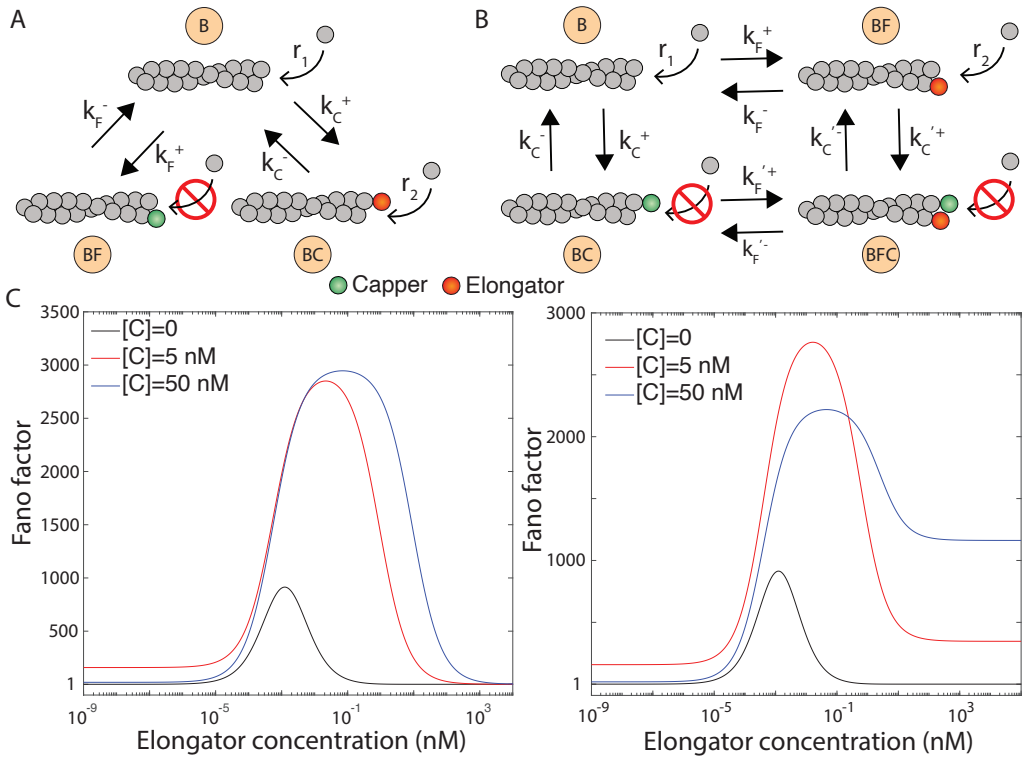

Figure 4. **Combined effect of a capper and an elongator on actin filament length.** (A) Competitive and (B) simultaneous binding models are shown. (C) Fano factor in steady-state is shown as a function of elongator concentration for various capper concentrations. Steady-state plots are generated for a fixed time window, $\tau = 100s$. Following parameters for elongator (formin) and capper (capping protein) are used: $r_1 = 6$ subunits/s, $r_2 = 30$ subunits/s, $\widetilde{k_F^+} = 29.1\ \mu M^{-1}s^{-1}$, $k_F^- = 8.1 \times 10^{-5}\ s^{-1}$, $\widetilde{k_C^+} = 12.8\ \mu M^{-1}s^{-1}$ $k_C^- = 2.0 \times 10^{-4}\ s^{-1}$, $\widetilde{k_F'^+} = 1.6\ \mu M^{-1}s^{-1}$, $\widetilde{k_C'^+} = 0.21\ \mu M^{-1}s^{-1}$, and $k_F'^- = k_C'^- = 6.2 \times 10^{-3}\ s^{-1}$ [19].

Fellowship.

[1] P. Lappalainen, T. Kotila, A. Jegou, and G. Romet-Lemonne. Biochemical and mechanical regulation of actin dynamics. *Nat Rev Mol Cell Biol*, 23(12):836–852, 2022.

[2] T. D. Pollard and G. G. Borisy. Cellular motility driven by assembly and disassembly of actin filaments. *Cell*, 112(4):453–65, 2003.

[3] M. F. Carlier and S. Shekhar. Global treadmilling coordinates actin turnover and controls the size of actin networks. *Nat Rev Mol Cell Biol*, 18(6):389–401, 2017.

[4] S. Romero, C. Le Clainche, D. Didry, C. Egile, D. Pantaloni, and M. F. Carlier. Formin is a processive motor that requires profilin to accelerate actin assembly and associated atp hydrolysis. *Cell*, 119(3):419–29, 2004.

[5] D. R. Kovar, E. S. Harris, R. Mahaffy, H. N. Higgs, and T. D. Pollard. Control of the assembly of atp- and adp-actin by formins and profilin. *Cell*, 124(2):423–35, 2006.

[6] D. A. Schafer, P. B. Jennings, and J. A. Cooper. Dynamics of capping protein and actin assembly in vitro: uncapping barbed ends by polyphosphoinositides. *J Cell Biol*, 135(1):169–79, 1996.

[7] S. Shekhar and M. F. Carlier. Enhanced depolymerization of actin filaments by adf/cofilin and monomer funneling by capping protein cooperate to accelerate barbed-end growth. *Curr Biol*, 27(13):1990–1998 e5, 2017.

[8] H. Wioland, B. Guichard, Y. Senju, S. Myram, P. Lappalainen, A. Jegou, and G. Romet-Lemonne. Adf/cofilin accelerates actin dynamics by severing filaments and promoting their depolymerization at both ends. *Curr Biol*, 27(13):1956–1967 e7, 2017.

[9] M. F. Carlier, V. Laurent, J. Santolini, R. Melki, D. Didry, G. X. Xia, Y. Hong, N. H. Chua, and D. Pantaloni. Actin depolymerizing factor (adf/cofilin) enhances the rate of filament turnover: implication in actin-based motility. *J Cell Biol*, 136(6):1307–22, 1997.

[10] A. Jegou, T. Niedermayer, J. Orban, D. Didry, R. Lipowsky, M. F. Carlier, and G. Romet-Lemonne. Individual actin

filaments in a microfluidic flow reveal the mechanism of atp hydrolysis and give insight into the properties of profilin. *PLoS Biol*, 9(9):e1001161, 2011.

[11] Romet-Lemonne G Wioland H, Jégou A. Celebrating 20 years of live single-actin-filament studies with five golden rules. *Proc Natl Acad Sci U S A*, 119:e2109506119, 2022.

[12] H. Ulrichs, I. Gaska, and S. Shekhar. Multicomponent regulation of actin barbed end assembly by twinfilin, formin and capping protein. *Nat Commun*, 14(1):3981, 2023.

[13] Ankita Arya, Sandeep Choubey, and Shashank Shekhar. Actin filament barbed-end depolymerization by combined action of profilin, cofilin, and twinfilin. *PRX Life*, 2:033002, Jul 2024.

[14] R. W. Pan, T. Röschinger, K. Faizi, H. Garcia, and R. Phillips. Deciphering regulatory architectures from synthetic single-cell expression patterns. *arXiv*, 2024.

[15] Goode BL. Breitsprecher D. Formins at a glance. *J Cell Sci*, Pt 1:1–7, 2013.

[16] M. Edwards, A. Zwolak, D. A. Schafer, D. Sept, R. Dominguez, and J. A. Cooper. Capping protein regulators fine-tune actin assembly dynamics. *Nat Rev Mol Cell Biol*, 15(10):677–89, 2014.

[17] S. Shekhar, M. Kerleau, S. Kuhn, J. Pernier, G. Romet-Lemonne, A. Jegou, and M. F. Carlier. Formin and capping protein together embrace the actin filament in a menage a trois. *Nat Commun*, 6:8730, 2015.

[18] J. P. Bombardier, J. A. Eskin, R. Jaiswal, Jr. Correa, I. R., M. Q. Xu, B. L. Goode, and J. Gelles. Single-molecule visualization of a formin-capping protein 'decision complex' at the actin filament barbed end. *Nat Commun*, 6:8707, 2015.

[19] S. Shekhar, M. Kerleau, S. Kühn, J. Pernier, G. Romet-Lemonne, A. Jégou, and M. F. Carlier. Formin and capping protein together embrace the actin filament in a ménage à trois. *Nat. Commun.*, 6:8730, 2015.

[20] E. M. Towsif, B. A. Miller, H. Ulrichs, and S. Shekhar. Multicomponent depolymerization of actin filament pointed ends by cofilin and cyclase-associated protein depends upon filament age. *Eur. J. .Cell Biol.*, 103:151423, 2024.

[21] H. Ulrichs, I. Gaska, and S. Shekhar. Multicomponent regulation of actin barbed end assembly by twinfilin, formin and capping protein. *Nat. Commun.*, 14:3981–3981, 2023.

[22] L. Mohapatra, B. L. Goode, and J. Kondev. Antenna mechanism of length control of actin cables. *PLOS Computational Biology*, 11:1–16, 2015.

[23] L. Mohapatra, B. L. Goode, P. Jelenkovic, R. Phillips, and J. Kondev. Design principles of length control of cytoskeletal structures. *Annual Review of Biophysics*, 45:85–116, 2016.

[24] D. S. Banerjee and S. Banerjee. Emergence and maintenance of variable-length actin filaments in a limiting pool of building blocks. *Biophys. J.*, 121:2436–2448, 2022.

[25] D. Johann, C. Erlenkämper, and K. Kruse. Length regulation of active biopolymers by molecular motors. *Phys. Rev. Lett.*, 108:258103, 2012.

[26] A. Matzavinos and H. G. Othmer. A stochastic analysis of actin polymerization in the presence of twinfilin and gelsolin. *J. Theor. Biol.*, 249:723–736, 2007.

[27] D Vavylonis, Q Yang, and B. O'Shaughnessy. Actin polymerization kinetics, cap structure, and fluctuations. *Proc. Natl. Acad. Sci.*, 102(24):8543–8548, 2005.

[28] B. L. Goode, J. Eskin, and S. Shekhar. Mechanisms of actin disassembly and turnover. *J Cell Biol*, 222(12), 2023.

[29] Rottner K. Faix J. Ena/vasp proteins in cell edge protrusion, migration and adhesion. *J Cell Sci*, 135:1–7, 2022.

Supplymentary material for A generalized theoretical framework to investigate multicomponent actin dynamics

Mintu Nandi, Shashank Shekhar, Sandeep Choubey

1 Moments of actin filament length distribution in the presence of an arbitrary number of actin binding proteins

To compute all the moments of 1) filament length distributions as a function of time and 2) the steady-state distribution of filament lengths within a fixed time window, we use the master equation (1), as described in the main text. This equation can be exactly solved to obtain the n-th moment of the distribution of ΔL_t as a function of time and ΔL_τ. To compute the transient moments, we define the following vectors of partial moments,

$$\begin{aligned}\overrightarrow{\Delta L_t^{(0)}} &= \sum_{\Delta L_t=-\infty}^{\infty} \Delta L_t^0 \mathbf{P}(\Delta L_t) \\ &= \left(\sum_{\Delta L_t=-\infty}^{\infty} P_1(\Delta L_t), \quad \cdots, \quad \sum_{\Delta L_t=-\infty}^{\infty} P_{N_1}(\Delta L_t), \quad \sum_{\Delta L_t=-\infty}^{\infty} P_{N_1+1}(\Delta L_t), \quad \cdots, \quad \sum_{\Delta L_t=-\infty}^{\infty} P_N(\Delta L_t) \right)^T, \end{aligned} \tag{S1}$$

$$\begin{aligned}\overrightarrow{\Delta L_t^{(n)}} &= \sum_{\Delta L_t=-\infty}^{\infty} \Delta L_t^n \mathbf{P}(\Delta L_t) \\ &= \left(\sum_{\Delta L_t=-\infty}^{\infty} \Delta L_t^n P_1(\Delta L_t), \quad \cdots, \quad \sum_{\Delta L_t=-\infty}^{\infty} \Delta L_t^n P_{N_1}(\Delta L_t), \quad \sum_{\Delta L_t=-\infty}^{\infty} \Delta L_t^n P_{N_1+1}(\Delta L_t), \quad \cdots, \right. \\ &\qquad \left. \sum_{\Delta L_t=-\infty}^{\infty} \Delta L_t^n P_N(\Delta L_t) \right)^T. \end{aligned} \tag{S2}$$

In Eq. (S1), $\sum_{\Delta L_t=-\infty}^{\infty} P_i(\Delta L_t)$ represents the probability of occurrence of filament state i (i.e., state visit probability). In Eq. (S2), $\sum_{\Delta L_t=-\infty}^{\infty} \Delta L_t^n P_i(\Delta L_t)$ stands for the n^{th} partial moment due to the state i. These vectors are instrumental in calculating the moments of the probability distribution of the change in length of the filament. For instance, the n^{th} central moment can be expressed as the sum of all elements of the vector $\overrightarrow{\Delta L_t^{(n)}}$, i.e.,

$$\langle \Delta L_t^n \rangle = \sum_{i=1}^{N} \left(\overrightarrow{\Delta L_t^{(n)}} \right)_{i1} = \overrightarrow{Y} . \overrightarrow{\Delta L_t^{(n)}}, \tag{S3}$$

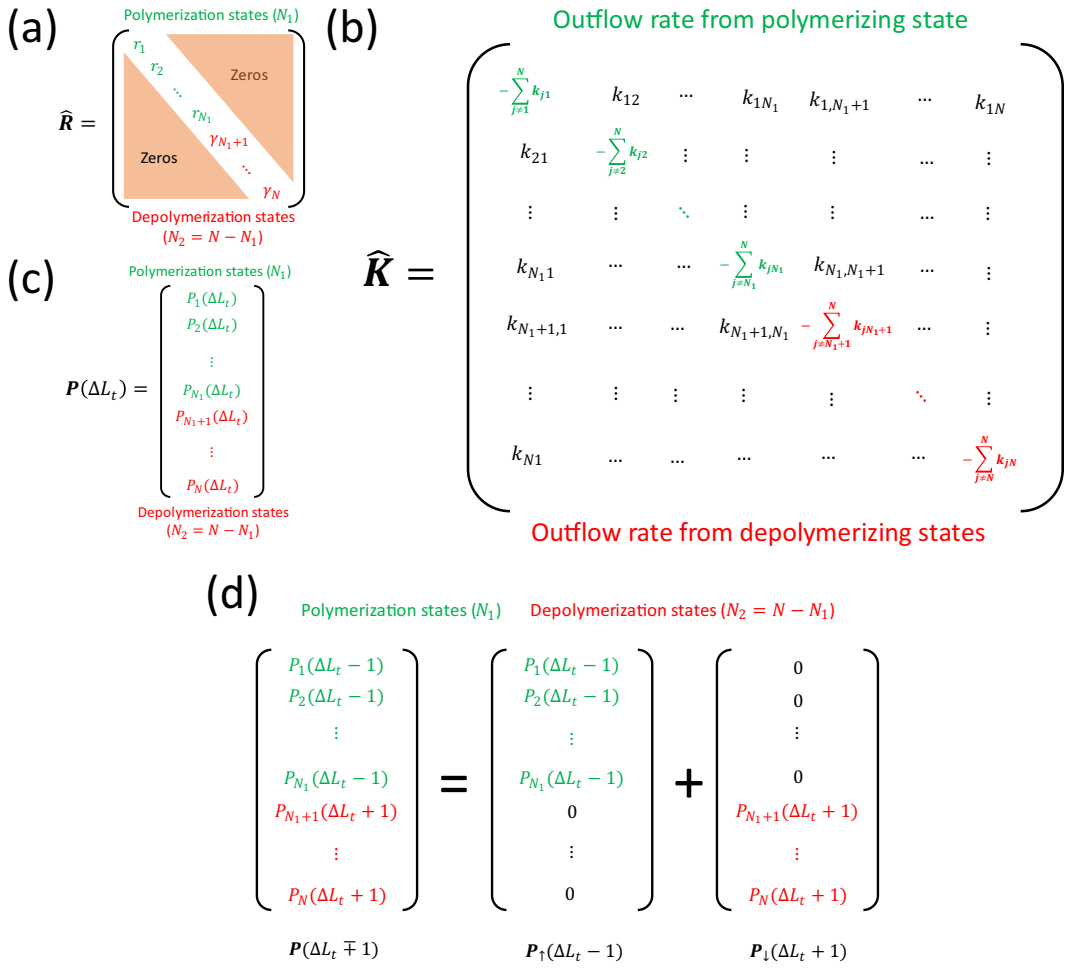

Figure S1: The schematics of structures of the matrices (a) $\hat{\mathbf{R}}$, (b) $\hat{\mathbf{K}}$, and (c) $\mathbf{P}(\Delta L_t)$. (d) The decomposition of transition probability vector.

where $\overrightarrow{Y} = (1,\ 1,\ \cdots,\ 1)_{(1\times N)}$. We note that $\overrightarrow{Y} \cdot \overrightarrow{\Delta L_t^{(0)}} = 1$, as the total state visit probability must always equal unity. To calculate $\overrightarrow{\Delta L_t^{(n)}}$, both sides of master equation (1) are multiplied by ΔL_t^n, followed by summing over all values of ΔL_t, which results in

$$\begin{aligned}\frac{d}{dt}\overrightarrow{\Delta L_t^{(n)}} &= \sum_{\Delta L_t=-\infty}^{\infty} \Delta L_t^n \frac{d}{dt}\mathbf{P}(\Delta L_t), \\ &= \left(\hat{\mathbf{K}} - \hat{\mathbf{R}}\right)\overrightarrow{\Delta L_t^{(n)}} + \hat{\mathbf{R}}\left[\sum_{\Delta L_t^{=}-\infty}^{\infty}(1+\Delta L_t)^n \mathbf{P}_{\uparrow}(\Delta L_t) + \sum_{\Delta L_t=-\infty}^{\infty}(-1)^n(1-\Delta L_t)^n \mathbf{P}_{\downarrow}(\Delta L_t)\right]. \quad \text{(S4)}\end{aligned}$$

In deriving Eq. (S4), we have employed the change of variable $\Delta L_t - 1 \to \Delta L_t'$ and $\Delta L_t + 1 \to \Delta L_t''$ followed by revert back to ΔL_t for notational simplicity. We define the binomial expansions $(1+\Delta L_t)^n = \sum_{x=0}^{n}\binom{n}{x}\Delta L_t^x =$

$1+\sum_{x=1}^{n}\binom{n}{x}\Delta L_t^x$ and $(1-\Delta L_t)^n=\sum_{x=0}^{n}(-1)^x\binom{n}{x}\Delta L_t^x=1+\sum_{x=1}^{n}(-1)^x\binom{n}{x}\Delta L_t^x$, where $\binom{n}{x}=n!/(x!(n-x)!)$ is called binomial coefficient. Employing the binomial expansion on Eq. (S4) yields,

$$\begin{aligned}\frac{d}{dt}\overrightarrow{\Delta L_t^{(n)}} &= \left(\hat{\mathbf{K}}-\hat{\mathbf{R}}\right)\overrightarrow{\Delta L_t^{(n)}}+\hat{\mathbf{R}}\sum_{\Delta L_t^{=}-\infty}^{\infty}\left(1+\sum_{x=1}^{n}\binom{n}{x}\Delta L_t^x\right)\mathbf{P}_{\uparrow}(\Delta L_t)\\ &+\hat{\mathbf{R}}\sum_{\Delta L_t=-\infty}^{\infty}(-1)^n\left(1+\sum_{x=1}^{n}(-1)^x\binom{n}{x}\Delta L_t^x\right)\mathbf{P}_{\downarrow}(\Delta L_t).\end{aligned}\tag{S5}$$

We now define $\overrightarrow{\Delta L_{t_\uparrow}^{(0)}}=\sum_{\Delta L_t=-\infty}^{\infty}\mathbf{P}_{\uparrow}(\Delta L_t)$ and $\overrightarrow{\Delta L_{t_\downarrow}^{(0)}}=\sum_{\Delta L_t=-\infty}^{\infty}\mathbf{P}_{\downarrow}(\Delta L_t)$ as the state visit probabilities from polymerizing and depolymerizing states, respectively. This gives $\overrightarrow{\Delta L_t^{(0)}}=\overrightarrow{\Delta L_{t_\uparrow}^{(0)}}+\overrightarrow{\Delta L_{t_\downarrow}^{(0)}}$. Again, the n^{th} partial moment vector follow the similar relation, i.e., $\overrightarrow{\Delta L_t^{(n)}}=\overrightarrow{\Delta L_{t_\uparrow}^{(n)}}+\overrightarrow{\Delta L_{t_\downarrow}^{(n)}}$, where partial moment vector due to polymerizing and depolymerizing states are defined as, $\overrightarrow{\Delta L_{t_\uparrow}^{(n)}}=\sum_{\Delta L_t=-\infty}^{\infty}\Delta L_t^n\mathbf{P}_{\uparrow}(\Delta L_t)$ and $\overrightarrow{\Delta L_{t_\downarrow}^{(n)}}=\sum_{\Delta L_t=-\infty}^{\infty}\Delta L_t^n\mathbf{P}_{\downarrow}(\Delta L_t)$, respectively. Using these definitions, we rearrange Eq. (S5) as,

$$\frac{d}{dt}\overrightarrow{\Delta L_t^{(n)}} = \hat{\mathbf{K}}\overrightarrow{\Delta L_t^{(n)}}+\hat{\mathbf{R}}\left[\overrightarrow{\Delta L_{t_\uparrow}^{(0)}}+(-1)^n\overrightarrow{\Delta L_{t_\downarrow}^{(0)}}\right]+\hat{\mathbf{R}}\sum_{x=1}^{n-1}\binom{n}{x}\left[\overrightarrow{\Delta L_{t_\uparrow}^{(x)}}+(-1)^{n+x}\overrightarrow{\Delta L_{t_\downarrow}^{(x)}}\right].\tag{S6}$$

We multiply both sides of Eq. (S6) by $\overrightarrow{Y}$ and use Eq. (S3), which leads to

$$\frac{d}{dt}\langle\Delta L_t^n\rangle=\overrightarrow{R}\left[\overrightarrow{\Delta L_{t_\uparrow}^{(0)}}+(-1)^n\overrightarrow{\Delta L_{t_\downarrow}^{(0)}}\right]+\overrightarrow{R}\sum_{x=1}^{n-1}\binom{n}{x}\left[\overrightarrow{\Delta L_{t_\uparrow}^{(x)}}+(-1)^{n+x}\overrightarrow{\Delta L_{t_\downarrow}^{(x)}}\right],\tag{S7}$$

where, following the definition of matrices $\hat{\mathbf{K}}$ and $\hat{\mathbf{R}}$, we arrive at $\overrightarrow{Y}.\hat{\mathbf{K}}=0$ and $\overrightarrow{R}=\overrightarrow{Y}.\hat{\mathbf{R}}$ where $\overrightarrow{R}$ represents a row vector containing the diagonal elements of $\hat{\mathbf{R}}$. Eq. (S7) forms the n^{th} moment equation. Solving Eq. (S7) yields the expression of n^{th} central moment for ΔL_t, provided we have the explicit expressions of $\overrightarrow{\Delta L_{t_\uparrow}^{(0)}}$, $\overrightarrow{\Delta L_{t_\downarrow}^{(0)}}$, $\overrightarrow{\Delta L_{t_\uparrow}^{(x)}}$, and $\overrightarrow{\Delta L_{t_\downarrow}^{(x)}}$. To solve this moment equation, we utilize the Laplace transformation with the initial condition that $\langle\Delta L_{t=0}^n\rangle=0$, reflecting the fact that filament elongation or shortening has not started yet at initial times. This approach leads to the following expression

$$\langle\Delta L_s^n\rangle = \frac{1}{s}\overrightarrow{R}\left[\overrightarrow{\Delta L_{s_\uparrow}^{(0)}}+(-1)^n\overrightarrow{\Delta L_{s_\downarrow}^{(0)}}\right]+\frac{1}{s}\overrightarrow{R}\sum_{x=1}^{n-1}\binom{n}{x}\left[\overrightarrow{\Delta L_{s_\uparrow}^{(x)}}+(-1)^{n+x}\overrightarrow{\Delta L_{s_\downarrow}^{(x)}}\right].\tag{S8}$$

To find $\overrightarrow{\Delta L_{s_\uparrow}^{(0)}}$ and $\overrightarrow{\Delta L_{s_\downarrow}^{(0)}}$ associated with Eq.(S8), we begin by computing the equation for $\overrightarrow{\Delta L_t^{(0)}}$ by summing master equation (1) over all values of ΔL_t. This results in

$$\frac{d}{dt}\overrightarrow{\Delta L_t^{(0)}} = \sum_{\Delta L_t=-\infty}^{\infty}\frac{d}{dt}\mathbf{P}(\Delta L_t)=\hat{\mathbf{K}}\overrightarrow{\Delta L_t^{(0)}}.\tag{S9}$$

While deriving Eq. (S9), we use the change of variable $\Delta L_t-1\rightarrow\Delta L_t'$ and $\Delta L_t+1\rightarrow\Delta L_t''$. Solving Eq. (S9) in Laplace domain with the initial condition that at the initial time, the filament exists in state 1 (free state) which yields $\overrightarrow{\Delta L_{t=0}^{(0)}}=(1\ 0\ \cdots\ 0)^T=\overrightarrow{I}$. This operation results in,

$$\begin{aligned}\overrightarrow{\Delta L_s^{(0)}} &= (s\hat{\mathbf{I}}-\hat{\mathbf{K}})^{-1}\overrightarrow{I},\\ \overrightarrow{\Delta L_{s_\uparrow}^{(0)}}+\overrightarrow{\Delta L_{s_\downarrow}^{(0)}} &= (s\hat{\mathbf{I}}-\hat{\mathbf{K}})^{-1}\overrightarrow{I}\end{aligned}\tag{S10}$$

where $\hat{\mathbf{I}}$ stands for the identity matrix. Now, it is important to decompose the vector obtained from the matrix operation of the right-hand side of Eq. (S10) and must correspond to the decomposition of $\mathbf{P}(\Delta L_t \mp 1)$ (see Fig. S1d). The decomposition of $(s\hat{\mathbf{I}} - \hat{\mathbf{K}})^{-1}\overrightarrow{I}$ results in two vectors: one has non-zero values of the elements for polymerizing states and zero values for depolymerizing states, which provides the expression of $\overrightarrow{\Delta L}^{(0)}_{s_\uparrow}$. On the contrary, the second vector contains zero values of the elements for polymerizing states and non-zero values for depolymerizing states, resulting in $\overrightarrow{\Delta L}^{(0)}_{s_\downarrow}$. As the general matrix forms of $\overrightarrow{\Delta L}^{(0)}_{s_\uparrow}$ and $\overrightarrow{\Delta L}^{(0)}_{s_\downarrow}$ are difficult to show, the computation of these two vectors has been performed using suitable software.

To compute $\overrightarrow{\Delta L}^{(x)}_{s_\uparrow}$ and $\overrightarrow{\Delta L}^{(x)}_{s_\downarrow}$, we derive the equation for $\overrightarrow{\Delta L}^{(x)}_{t}$ by rewriting Eq. (S6) in terms of x^{th} partial moment equation as,

$$\frac{d}{dt}\overrightarrow{\Delta L}^{(x)}_{t} = \hat{\mathbf{K}}\overrightarrow{\Delta L}^{(x)}_{t} + \hat{\mathbf{R}}\left[\overrightarrow{\Delta L}^{(0)}_{t_\uparrow} + (-1)^n\overrightarrow{\Delta L}^{(0)}_{t_\downarrow}\right] + \hat{\mathbf{R}}\sum_{z=1}^{x-1}\binom{x}{z}\left[\overrightarrow{\Delta L}^{(z)}_{t_\uparrow} + (-1)^{x+z}\overrightarrow{\Delta L}^{(z)}_{t_\downarrow}\right]. \tag{S11}$$

Upon Laplace transformation with the initial condition that at $t = 0$ the partial moments are zero, i.e., $\overrightarrow{\Delta L}^{(x)}_{t=0} = 0$, Eq. (S11) results in,

$$\begin{aligned}
\overrightarrow{\Delta L}^{(x)}_{s} &= (s\hat{\mathbf{I}} - \hat{\mathbf{K}})^{-1}\hat{\mathbf{R}}\left[\overrightarrow{\Delta L}^{(0)}_{s_\uparrow} + (-1)^x\overrightarrow{\Delta L}^{(0)}_{s_\downarrow}\right] + (s\hat{\mathbf{I}} - \hat{\mathbf{K}})^{-1}\hat{\mathbf{R}}\sum_{z=1}^{x-1}\binom{x}{z}\left[\overrightarrow{\Delta L}^{(z)}_{s_\uparrow} + (-1)^{x+z}\overrightarrow{\Delta L}^{(z)}_{s_\downarrow}\right], \\
\overrightarrow{\Delta L}^{(x)}_{s_\uparrow} + \overrightarrow{\Delta L}^{(x)}_{s_\downarrow} &= (s\hat{\mathbf{I}} - \hat{\mathbf{K}})^{-1}\hat{\mathbf{R}}\left[\overrightarrow{\Delta L}^{(0)}_{s_\uparrow} + (-1)^x\overrightarrow{\Delta L}^{(0)}_{s_\downarrow}\right] + (s\hat{\mathbf{I}} - \hat{\mathbf{K}})^{-1}\hat{\mathbf{R}}\sum_{z=1}^{x-1}\binom{x}{z}\left[\overrightarrow{\Delta L}^{(z)}_{s_\uparrow} + (-1)^{x+z}\overrightarrow{\Delta L}^{(z)}_{s_\downarrow}\right],
\end{aligned} \tag{S12}$$

We know that $\overrightarrow{\Delta L}^{(x)}_{t} = \overrightarrow{\Delta L}^{(x)}_{t_\uparrow} + \overrightarrow{\Delta L}^{(x)}_{t_\downarrow}$ are also true in Laplace domain. Using this equality and following the previously stated decomposition of $\overrightarrow{\Delta L}^{(0)}_{t}$, we compute the right-hand side of Eq. (S12), which yields a vector of dimension $N \times 1$. We then decompose this vector into polymerizing and depolymerizing components: in the polymerizing vector, the first N_1 elements are non-zero and the remaining N_2 elements are zero; conversely, in the depolymerizing vector, the first N_1 elements are set to zero and the next N_2 elements are non-zero. This method of decomposition yields $\overrightarrow{\Delta L}^{(x)}_{t_\uparrow}$ and $\overrightarrow{\Delta L}^{(x)}_{t_\downarrow}$.

Eq. (S8) together with Eqs. (S10) and (S12) compute the expression of n^{th} central moment in the Laplace domain. We write the expression of time-dependent n^{th} central moment of the change in length of the filament by performing inverse Laplace transformation on Eq. (S8), which gives

$$\langle \Delta L_t^n \rangle = \overrightarrow{R}\left[\overrightarrow{\Lambda}^{(0)}_{t_\uparrow} + (-1)^n\overrightarrow{\Lambda}^{(0)}_{t_\downarrow}\right] + \overrightarrow{R}\sum_{x=1}^{n-1}\binom{n}{x}\left[\overrightarrow{\Lambda}^{(x)}_{t_\uparrow} + (-1)^{n+x}\overrightarrow{\Lambda}^{(x)}_{t_\downarrow}\right], \tag{S13}$$

where, $\overrightarrow{\Lambda}^{(0)}_{t_\uparrow} = \mathcal{L}^{-1}\left[\overrightarrow{\Delta L}^{(0)}_{s_\uparrow}/s\right]$, $\overrightarrow{\Lambda}^{(0)}_{t_\downarrow} = \mathcal{L}^{-1}\left[\overrightarrow{\Delta L}^{(0)}_{s_\downarrow}/s\right]$, $\overrightarrow{\Lambda}^{(x)}_{t_\uparrow} = \mathcal{L}^{-1}\left[\overrightarrow{\Delta L}^{(x)}_{s_\uparrow}/s\right]$, and $\overrightarrow{\Lambda}^{(x)}_{t_\downarrow} = \mathcal{L}^{-1}\left[\overrightarrow{\Delta L}^{(x)}_{s_\downarrow}/s\right]$. Here, the symbol $\mathcal{L}^{-1}$ is used to refer the inverse Laplace transformation.

To compute the steady-state moments of actin length distribution, we begin by setting the left-hand side of Eq. (S9) to zero as the probabilities of visiting different states become independent of time and we denote it as $\overrightarrow{\Delta L}^{(0)}$. Additionally, the sum of state visit probabilities will be unity at steady-state. Mathematically, we express

these two conditions as,

$$\hat{\mathbf{K}}.\overrightarrow{\Delta L}^{(0)} = 0, \tag{S14}$$

$$\overrightarrow{Y}.\overrightarrow{\Delta L}^{(0)} = 1. \tag{S15}$$

On solving these two coupled equations, the state visit probability vector $\overrightarrow{\Delta L}^{(0)}$ is computed. We decompose $\overrightarrow{\Delta L}^{(0)}$ into two partial vectors: one is the polymerizing vector, $\overrightarrow{\Delta L}^{(0)}_{\uparrow}$, where the first N_1 elements are non-zero and the remaining N_2 elements are zero, and second the depolymerizing vector $\overrightarrow{\Delta L}^{(0)}_{\downarrow}$, where the first N_1 elements are zero and the next N_2 elements are non-zero. We have used this method of decomposition in the case of deriving temporal moments.

We now replace the time variable t with τ in Eq. (S7) and perform Laplace transformation on both sides of the equation with the initial condition that $\langle \Delta L^n_{t\to\infty}\rangle\big|_\tau = 0$. This initial condition is chosen to track the change in length of the filament that occurs within the window from t to $t+\tau$, excluding any change in length that occurred up to time t. These operations lead to

$$\langle \Delta L^n_s\rangle\big|_\tau = \frac{1}{s^2}\overrightarrow{R}\left[\overrightarrow{\Delta L}^{(0)}_{\uparrow} + (-1)^n\overrightarrow{\Delta L}^{(0)}_{\downarrow}\right] + \frac{1}{s}\overrightarrow{R}\sum_{x=1}^{n-1}\binom{n}{x}\left[\overrightarrow{\Delta L}^{(x)}_{s_\uparrow}\big|_\tau + (-1)^{n+x}\overrightarrow{\Delta L}^{(x)}_{s_\downarrow}\big|_\tau\right], \tag{S16}$$

where, the terms $\overrightarrow{\Delta L}^{(0)}_{\uparrow}$ and $\overrightarrow{\Delta L}^{(0)}_{\downarrow}$ are known from Eqs. (S14-S15). The unknown quantities $\overrightarrow{\Delta L}^{(x)}_{s_\uparrow}\big|_\tau$ and $\overrightarrow{\Delta L}^{(x)}_{s_\downarrow}\big|_\tau$ are computed by evaluating Eq. (S11) at steady-state and we then perform Laplace transformation with the initial condition that $\overrightarrow{\Delta L}^{(x)}_{t\to\infty}\big|_\tau = 0$. This results in,

$$\begin{aligned}
\overrightarrow{\Delta L}^{(x)}_{s}\big|_\tau &= \frac{1}{s}(s\hat{\mathbf{I}}-\hat{\mathbf{K}})^{-1}\hat{\mathbf{R}}\left[\overrightarrow{\Delta L}^{(0)}_{\uparrow} + (-1)^n\overrightarrow{\Delta L}^{(0)}_{\downarrow}\right] \\
&\quad +(s\hat{\mathbf{I}}-\hat{\mathbf{K}})^{-1}\hat{\mathbf{R}}\sum_{z=1}^{x-1}\binom{x}{z}\left[\overrightarrow{\Delta L}^{(x)}_{s_\uparrow}\big|_\tau + (-1)^{n+x}\overrightarrow{\Delta L}^{(x)}_{s_\downarrow}\big|_\tau\right], \\
\overrightarrow{\Delta L}^{(x)}_{s_\uparrow}\big|_\tau + \overrightarrow{\Delta L}^{(x)}_{s_\downarrow}\big|_\tau &= \frac{1}{s}(s\hat{\mathbf{I}}-\hat{\mathbf{K}})^{-1}\hat{\mathbf{R}}\left[\overrightarrow{\Delta L}^{(0)}_{\uparrow} + (-1)^n\overrightarrow{\Delta L}^{(0)}_{\downarrow}\right] \\
&\quad +(s\hat{\mathbf{I}}-\hat{\mathbf{K}})^{-1}\hat{\mathbf{R}}\sum_{z=1}^{x-1}\binom{x}{z}\left[\overrightarrow{\Delta L}^{(x)}_{s_\uparrow}\big|_\tau + (-1)^{n+x}\overrightarrow{\Delta L}^{(x)}_{s_\downarrow}\big|_\tau\right].
\end{aligned} \tag{S17}$$

The decomposition of partial moment vector also applies to steady-state scenario. Using this decomposition, we have $\overrightarrow{\Delta L}^{(x)}_{s}\big|_\tau = \overrightarrow{\Delta L}^{(x)}_{s_\uparrow}\big|_\tau + \overrightarrow{\Delta L}^{(x)}_{s_\downarrow}\big|_\tau$. We now decompose the resultant vector obtained from the right-hand side of Eq. (S17), yielding two partial vectors: one corresponds to $\overrightarrow{\Delta L}^{(x)}_{s_\uparrow}\big|_\tau$ where the first N_1 elements are non-zero but the next N_2 elements are zero, and the second $\overrightarrow{\Delta L}^{(x)}_{s_\downarrow}\big|_\tau$, where the first N_1 elements are zero but the next N_2 elements are non-zero. Performing inverse Laplace transform of Eq. (S16) with the help of Eq. (S17), we have the n^{th} central moment as a function of time window τ,

$$\langle \Delta L^n_\tau\rangle = \overrightarrow{R}\left[\overrightarrow{\Delta L}^{(0)}_{\uparrow} + (-1)^n\overrightarrow{\Delta L}^{(0)}_{\downarrow}\right]\tau + \overrightarrow{R}\sum_{x=1}^{n-1}\binom{n}{x}\left[\overrightarrow{\Lambda}^{(x)}_{\tau_\uparrow} + (-1)^{n+x}\overrightarrow{\Lambda}^{(x)}_{\tau_\downarrow}\right], \tag{S18}$$

where, $\overrightarrow{\Lambda}^{(x)}_{\tau_\uparrow} = \mathcal{L}^{-1}\left[\frac{\overrightarrow{\Delta L}^{(x)}_{s_\uparrow}\big|_\tau}{s}\right]$ and $\overrightarrow{\Lambda}^{(x)}_{\tau_\downarrow} = \mathcal{L}^{-1}\left[\frac{\overrightarrow{\Delta L}^{(x)}_{s_\downarrow}\big|_\tau}{s}\right]$.

Note that such master equation-based models have been employed in other fields of single-molecule biology to study their governing principles [1, 2, 3].

2 Moments of actin length distribution regulated by an elongator

In the presence of an elongator, the governing master equations are,

$$\frac{dP_B(\Delta L_t)}{dt} = -k_F^+ P_B(\Delta L_t) + k_F^- P_{BF}(\Delta L_t) - r_1 P_B(\Delta L_t) + r_1 P_B(\Delta L_t - 1), \tag{S19}$$

$$\frac{dP_{BF}(\Delta L_t)}{dt} = k_F^+ P_B(\Delta L_t) - k_F^- P_{BF}(\Delta L_t) - r_2 P_{BF}(\Delta L_t) + r_2 P_{BF}(\Delta L_t - 1). \tag{S20}$$

Expressing the above two equations in matrix form according to equation (1), we write the associated matrices as,
$\mathbf{P}(\Delta L_t) = \begin{pmatrix} P_B(\Delta L_t) \\ P_{BF}(\Delta L_t) \end{pmatrix}$, $\hat{\mathbf{K}} = \begin{pmatrix} -k_F^+ & k_F^- \\ k_F^+ & -k_F^- \end{pmatrix}$, and $\hat{\mathbf{R}} = \begin{pmatrix} r_1 & 0 \\ 0 & r_2 \end{pmatrix}$.

Using Eqs. (S13), we derive the corresponding moments (here we show up to the second moment) to obtain $\langle \Delta L_t \rangle$, $\langle \Delta L_t^2 \rangle$. Using the first and second moments, we express the variance of ΔL_t as $\sigma^2_{\Delta L_t} = \langle \Delta L_t^2 \rangle - \langle \Delta L_t \rangle^2$. The closed-form analytical expressions for mean change in length $\langle \Delta L_t \rangle$, variance $\sigma^2_{\Delta L_t}$ are given by

$$\langle \Delta L_t \rangle = r_1 A_F t + r_2(1 - A_F)t + \frac{(r_1 - r_2)(1 - A_F)}{D_F}(1 - e^{-D_F t}), \tag{S21}$$

$$\begin{aligned} \sigma^2_{\Delta L_t} = {} & \frac{(r_1 - r_2)(1 - A_F)\left[D_F + (r_1 - r_2)(1 - 5A_F)\right]}{D_F^2} + \left[r_2 + A_F(r_1 - r_2) + \frac{2A_F(1 - A_F)(r_1 - r_2)^2}{D_F}\right] t \\ & - \left[\frac{(1 - A_F)(r_1 - r_2)}{D_F}\right]^2 e^{-2D_F t} \\ & + \frac{(1 - A_F)(r_1 - r_2)}{D_F^2}\left[4A_F(r_1 - r_2) - D_F - 2D_F(1 - 2A_F)(r_1 - r_2)t\right] e^{-D_F t}, \end{aligned} \tag{S22}$$

where $D_F = k_F^+ + k_F^-$ and $A_F = k_F^-/D_F$.

Next, we compute the mean, variance at steady-state using Eq. (S18) and obtain $\langle \Delta L_\tau \rangle$, $\langle \Delta L_\tau^2 \rangle$. Using first and second central moments, we define the variance as $\sigma^2_{\Delta L_\tau} = \langle \Delta L_\tau^2 \rangle - \langle \Delta L_\tau \rangle^2$. The closed-form expressions of mean and variance are written as

$$\langle \Delta L_\tau \rangle = r_1 \tau + (r_1 - r_2) A_F \tau, \tag{S23}$$

$$\sigma^2_{\Delta L_\tau} = r_1 \tau + (r_1 - r_2) A_F \tau + \frac{2}{D_F}(r_1 - r_2)^2 A_F(1 - A_F)\tau - \frac{2}{D_F^2}(r_1 - r_2)^2 A_F(1 - A_F)(1 - e^{-\tau D_F}). \tag{S24}$$

3 Moments of actin length distribution regulated by a capper

The governing master equations for filament length in the presence of a capper is given by

$$\frac{dP_B(\Delta L_t)}{dt} = -k_C^+ P_B(\Delta L_t) + k_C^- P_{BC}(\Delta L_t) - r_1 P_B(\Delta L_t) + r_1 P_B(\Delta L_t - 1), \tag{S25}$$

$$\frac{dP_{BC}(\Delta L_t)}{dt} = k_C^+ P_B(\Delta L_t) - k_C^- P_{BC}(\Delta L_t). \tag{S26}$$

Expressing the above two equations in matrix form according to Eq. (**??**), the associated matrices are,
$\mathbf{P}(\Delta L_t) = \begin{pmatrix} P_B(\Delta L_t) \\ P_{BC}(\Delta L_t) \end{pmatrix}$, $\hat{\mathbf{K}} = \begin{pmatrix} -k_C^+ & k_C^- \\ k_C^+ & -k_C^- \end{pmatrix}$, and $\hat{\mathbf{R}} = \begin{pmatrix} r_1 & 0 \\ 0 & 0 \end{pmatrix}$.

Utilizing the general solution provided in Eqs. (S13), we derive the corresponding moments (up to the second moment) to obtain $\langle \Delta L_t \rangle$, and $\langle \Delta L_t^2 \rangle$. Using the first and second moments, we express the variance of ΔL_t as $\sigma^2_{\Delta L_t} = \langle \Delta L_t^2 \rangle - \langle \Delta L_t \rangle^2$. The closed-form analytical expressions for mean change in length $\langle \Delta L_t \rangle$, variance $\sigma^2_{\Delta L_t}$ are given by,

$$\langle \Delta L_t \rangle = r_1 A_C t + \frac{r_1(1-A_C)}{D_C}(1 - e^{-D_C t}), \tag{S27}$$

$$\sigma^2_{\Delta L_t} = r_1 A_C t + \frac{2r_1^2 A_C(1-A_C)t}{D_C} + \left[\frac{r_1(1-A_C)}{D_C}\right]^2 (1 - e^{-2D_C t}) + \frac{r_1(1-A_C)}{D_C}\left(1 - \frac{2r_1}{D_C}\right)(1 - e^{-D_C t}) + \frac{2r_1^2(1-A_C)(1-2A_C)}{D_C^2}\left[1 - (1 + D_C t)e^{-D_C t}\right], \tag{S28}$$

$$\tag{S29}$$

where $D_C = k_C^+ + k_C^-$ and $A_C = k_C^-/D_C$.

Next, we compute the mean, variance, and third central moment at steady-state using Eq. (S18) and obtain $\langle \Delta L_\tau \rangle$, and $\langle \Delta L_\tau^2 \rangle$. Using first and second central moments, we define the variance as $\sigma^2_{\Delta L_\tau} = \langle \Delta L_\tau^2 \rangle - \langle \Delta L_\tau \rangle^2$. The closed-form expressions of mean and variance are written as,

$$\langle \Delta L_\tau \rangle = r_1 A_C \tau, \tag{S30}$$

$$\sigma^2_{\Delta L_\tau} = r_1 A_C \tau + \frac{2}{D_C} r_1^2 A_C(1-A_C)\tau - \frac{2}{D_C^2} r_1^2 A_C(1-A_C)(1 - e^{-\tau D_C}). \tag{S31}$$

4 Moments of actin length distribution for competitive binding model and simultaneous binding models

4.1 Competitive binding model

In this model, the filament undergoes elongation from states B and BF with rates r_1 and r_2, respectively. To write the master equation according to Eq. (1) described in the main text, we define the following matrices,

$$\mathbf{P}(\Delta L_t) = \begin{pmatrix} P_B(\Delta L_t) \\ P_{BF}(\Delta L_t) \\ P_{BC}(\Delta L_t) \end{pmatrix}, \hat{\mathbf{K}} = \begin{pmatrix} -(k_F^+ + k_C^+) & k_F^- & k_C^- \\ k_F^+ & -k_F^- & 0 \\ k_C^+ & 0 & -k_C^- \end{pmatrix}, \text{ and } \hat{\mathbf{R}} = \begin{pmatrix} r_1 & 0 & 0 \\ 0 & r_2 & 0 \\ 0 & 0 & 0 \end{pmatrix}.$$

Using Eq. (S13), we derive the corresponding moments $\langle \Delta L_t \rangle$, and $\langle \Delta L_t^2 \rangle$. Using the first and second moments, the variance can be written as $\sigma^2_{\Delta L_t} = \langle \Delta L_t^2 \rangle - \langle \Delta L_t \rangle^2$. Due to the complexity of the analytical expressions, we don't report them here.

Next, we calculate the mean, variance, and third central moment at steady-state using Eq. (S18) to obtain $\langle \Delta L_\tau \rangle$, $\langle \Delta L_\tau^2 \rangle$, and $\langle \Delta L_\tau^3 \rangle$. Using first and second central moments, we define the variance as $\sigma^2_{\Delta L_\tau} = \langle \Delta L_\tau^2 \rangle - \langle \Delta L_\tau \rangle^2$. The closed form expressions of mean, variance are not reported here due to their complex expressions.

4.2 Simultaneous binding model

As described in the main text, in this model, the filament undergoes elongation from states B and BF with rates r_1 and r_2, respectively. To write the master equation according to Eq. (1) described in the main text, we define the following matrices,

$$\mathbf{P}(\Delta L_t) = \begin{pmatrix} P_B(\Delta L_t) \\ P_{BF}(\Delta L_t) \\ P_{BC}(\Delta L_t) \\ P_{BFC}(\Delta L_t) \end{pmatrix}, \hat{\mathbf{K}} = \begin{pmatrix} -(k_F^+ + k_C^+) & -k_F^- & k_C^- & 0 \\ k_F^+ & -(k_C'^+ + k_F^-) & 0 & k_C'^- \\ k_C^+ & 0 & -(k_F'^+ + k_C^-) & k_F'^- \\ 0 & k_C'^+ & k_F'^+ & -(k_F'^- + k_C'^-) \end{pmatrix},$$

and $\hat{\mathbf{R}} = \begin{pmatrix} r_1 & 0 & 0 & 0 \\ 0 & r_2 & 0 & 0 \\ 0 & 0 & 0 & 0 \\ 0 & 0 & 0 & 0 \end{pmatrix}$.

Using Eq. (S13), we derive the corresponding moments $\langle \Delta L_t \rangle$, and $\langle \Delta L_t^2 \rangle$. Using the first and second moments, the variance can be written as $\sigma^2_{\Delta L_t} = \langle \Delta L_t^2 \rangle - \langle \Delta L_t \rangle^2$. The closed form expressions of mean, variance are too cumbersome to be reported here.

Next, we calculate the mean, variance, and third central moment at steady-state using Eq. (S18) to obtain $\langle \Delta L_\tau \rangle$, and $\langle \Delta L_\tau^2 \rangle$. Using first and second central moments, we define the variance as $\sigma^2_{\Delta L_\tau} = \langle \Delta L_\tau^2 \rangle - \langle \Delta L_\tau \rangle^2$. The closed form expressions of mean, variance are too cumbersome to be reported here.

References

[1] N G van Kampen. *Stochastic Processes in Physics and Chemistry, 3rd ed.* North-Holland, Amsterdam, 2007.

[2] A. Sánchez and J. Kondev. Transcriptional control of noise in gene expression. *Proc. Natl. Acad. Sci., USA*, 105:5081–5086, 2008.

[3] S. Choubey. Nascent rna kinetics: Transient and steady state behavior of models of transcription. *Phys. Rev. E*, 97:022402, 2018.